Higher Order Cumulant Studies of Ocean Surface Random Fields from Satellite Altimeter Data

11(.!111 ty N. Cheng*

1. Introduction

Higher order statistics, especially 2nd order statistics, have been used to study ocean processes for many years in the past, and occupy an appreciable part of the research literature on physical oceanography. They in turn form part of a much larger field of study in statistical fluid mechanics (Monin and Yaglom 1975). With the advent of satellite remote sensing in oceanographic data collection in the 70's, II much of the higher order statistics popular with the signal processing community (Rosenblatt 1985; Nikias and Petropulu 1993) can and are now being applied to the stud y of the cart h's oceans. Some relevant papers on this subject are Fu (1 983), Glazman ( ] 986), LeTraon (1990). Since then, improvements in satellite technology have significantly reduced the error content of the collected data, resulting in better estimates of many important oceanic parameters such as sea surface height, wind speed, sea surface temperature, etc. An excellent Overview on recent applications of statistics in oceanography can be found in Chelton et al (1 994). Our purpose in this article is to report on some new applications of statistic] techniques in oceanography, primarily of the 2nd order, using some recently obtained satellite altimetry data, as well as raised some unanswered statistical problems for future study. Some glimpses into the applications of 3rd and higher order statistics are also provided for future research.

The TOPEX/Poseidon satellite is currently at the start of its 4th year of a 5 year

*Benny N Cheng is Statistician, Physical Oceanography Group, Jet Propulsion Laboratory, Pasadena, CA, 91109. This work was performed at the Jet Propulsion Laboratory, California Institute of Technology, under contract with the National Aeronautics and Space Administration. Financial support was provided by the Office of Naval Research. During this work, the author held a National Research Council-NASA-JPL Research Associateship. The author also thank Roman Glazman, Keh Shin Lee, Steve Elgar, and Alex Greysukh, for helpful comments in the preparation of this paper.

mission to map and study the world's ocean. A joint mission between the US and France, this satellite represents the state-of-the-art in oceanographic remote sensing technology. A main component of the data collected by this satellite is the sea surface height (SSH) of the ocean, which is accomplished with an onboard altimeter. This SS11 data is available to the public as a set of CDROMs produced in-house at the JPL-PODAAC group (Benada 1993). Using this data, we analyze the higher order cumulants of the SSH field and give some specific applications. Naturally, we will assume for the rest of this article that all moments exist and are finite. Readers who would like to improve their knowledge of oceanography may wish to consult the excellent books of Gill (1 982) and LeBlond and Mysak (1978).

2. Second Order Statistics

We begin by presenting an application of 2nd order statistic in oceanography. The ocean is a natural laboratory for the study of random processes, and until the recent advent of satellite remote sensing techniques, has had limited access to researchers. In the study of mesoscale events (from 10 km to 500 kin), oceanographic phenomena such as eddies, long gravity waves, and planetary waves are of great interest. They carry much of the energy stored in the ocean and act as natural capacitor or storage unit for the earth's energy budget. Such events are manifested in the variation of the oc.call sea surface height (SSH), which can be detected and measured with relatively good precision by a satellite altimeter. Further-more, duc to the fact that the ocean is not a uniform medium, the mass density of water differs at different depths, forming a stratification which allows internal waves to occur between interfaces of different densities. These internal waves can bc quite energetic, with amplitudes averaging 400 times that detected on the sea surface (Wunsch and Gill].976). Depending on the satellite speed, sampling rate, and spacing between orbits, certain types of waves are readily detect ed and their corresponding properties measured. Much of the literature in descriptive oceanography consists of visually interpreting the data, usually via a contour plot or a t ime series graph. A more sophisticated approach starts by

partitioning the ocean into square pa t ches not more than 10x] O degrees in size (a larger patch is less likely to be spatially homogeneous). The satellite ground tracks within a patch constitute a data set of SSH measurements, called the SS}1 random field or SSH field for snort. The sampling dist ance between points on a ground track is 6 km , and the satellite repeats its pass over the same track once every 10 days, and for this article, wc choose 73 consecutive passes wi rich gives a tot al of 73 (independent) realizations per track (about 2 years worth of data). This SSH field is thin, processed to remove unwanted errors such as sea state bias, inverse barometer effect, orbit cor rections. geoid corrections, tidal components, and finally the mean field is removed so as to insure a mean zero SSH field. It is claimed that the resulting estimate has a loot- mean- square er i or of 4,7 cm per pass (Fu et al 1994) and wc refer to their art icle r egarding the det ails of this preliminary processing of satellite altimeter data. To improve the accuracy further, we perfor m additional processing as follows:

(1) Passes with more than 2 consecutive bad or missing values are dropped. These account for less than 10 percent of the whole data set.

(2) SSH values greater than 30 cm ar e treated as bad values, and arc replaced with its linear interpolate whenever possible.

For a large number of patches, analysis of this r andom field shows it to be approximately homogeneous (Fu 1983; Le'Traon 1990) though not necessarily gaussian, which greatly simplifies the task of its decomposition into more fundamental components, The cumulants of this SSH field are of great interest to physical oceanographers, containing large amount of information about the st ructure of the embedded ocean waves. In particular, the 2nd order cumulants, or autocovar iance functions of SSH fields and its corresponding spectra obtained by applying FFT, have] Ire \'iousl y 1 oen used to study the properties of mesoscale variability both in the Atlantic (1 .e'Traon 1990) and the Pacific ocean (Glazman, Fabrikant, and Greysukh 1996, i n pr ess).

We now describe two important and distinct spatial autocovariance (or equivalently, autocorrelation) functions that can be computed from the SSH field. The first is called the along- track (AT) autocovariance function, which is named for the fact that spatial lags are taken along the path of the satellite's ground track. Lag intervals corresponds to the sampling interval of the satellite (6 km for TOPEX), which can be increased by subsampling the data. Furthermore, test satellites used in the earth sciences have exact orbit repeat period of several days (10 day cycle for TOPEX). Thus, to obtain a time-independent AT autocovariance function, we average the autocovariance function over all cycles. The calculations are done as follows: since the data is gridded with a constant spacing of 6 km between successive points, we partition a thousand kilometer lag space r into consecutive bins of size Δr= 6 km each, For each track in the patch, all SSH products with identical lags are collected and then averaged over all passes over this track. This procedure is then repeated for all subsequent tracks inside the patch, and the products summed together and divided by the number of points in each Δr bin. In mathematical notation, let $(x_{ijk}, y_{ijk}, z_{ijk})$ denote the ith point for pass j on track k, where (x, y) denote the coordinates of the point, and z is a realization of the SSH field at that point. Denote the sum of the product pairs with lag r by $S_{jk} = \{\sum_{i,i'} z_{ijk} z_{i'jk} : \mathrm{dist}(x_{ijk}, x_{i'jk}) = r\}$. Then

$$ATCov(r) = \sum_k \frac{\sum_j S_{jk}}{\sum_j 1} \Big/ \sum_{i,k} 1$$

This gives us the usual biased sample estimate of the one-dimensional (1-d) time-independent AT autocovariance function. As an illustration, we compute the AT autocovariance function of the SSH field and its power spectrum for a patch with coordinates longitude 330,340, latitude 30,40, situated in the North Atlantic ocean.

Figure 1 here

Other patches have a similar pattern, with slight differences that are oceanographic in nature and of no concern to us in this paper, hence all subsequent illustrations will be

based on this particular patch. The autocovariance function typically crosses the zero line around 150-200 km, corresponding to wavelengths about four times of the zero crossing value. The spectrum is computed by taking the FFT of the autocovariance function with the standard Hanning window. Specific details regarding the shape and features of the autocovariance and spectrum can be found in Fu (1983), Le Traon (1990), and Glazman et al (1996, in press). In particular, an interesting fact is that in the mid-region (from .02 to .07 rad/km) of the above log-log plot of the AT wave-number spectrum, the spectral slope generally lies between -2 and -3 , and has nearly the same shape for all parts of the world's oceans This spectral power law, analogous to the famous Kolmogorov's power law for turbulence, is theorized to be the consequence of a continuous energy transfer (or cascade) from lower wavenumbers to higher ones (Glazman 1996). Analogous power laws have been found earlier for smaller wavelength scales such as gravity and capillary waves, using data gathered from ships and various moored instruments (LeBlond anti Mysak 1978, p. 318; Phillips 1977, p. 336). The most recent theory (Glazman 1996) suggests that the AT wave-number spectrum is actually a composite of two different type of waves, shorter period (less than a day) inertia gravity waves and longer period (more than 10 days) planetary Rossby waves. To solve this decomposition problem, we are led to the estimation of the so-called between-track (BT) autocovariance function, which was first utilized to study SSH field in the paper by Glazman et al (1996, in press).

The principle behind the computation of the BT autocovariance function is to determine the contribution to the total spectrum of the SSH variations from waves having different time scales. This is accomplished by allocating spatial lag bins of size 20 km by 20 km square and dividing the total observation time into temporal lag bins of 5 days duration or more (also known in literature as a synchronicity interval (Glazman et al 1996, in press)). With the 5 days synchronicity interval, fast inertia gravity waves are decorrelated at this time scale, and their contributions to the SS11 spatial autocovariance function

become negligible, whereas contributions from the slower Rossby waves are dominant due to the fact that a 5 day time lag between any two observations is small compared with the characteristic period of Rossby waves. Data are collected for each of these spatio-temporal bins and averaged, and the autocovariance function computed. Since time coordinates as well as position of each sampled SSH point are recorded, it is relatively easy to compute this BT autocovariance as a function of time and a two dimensional lag plane. The only major drawback of this computation is the limited number of satellite tracks, usually between 9 to 12, within a patch. This corresponds to the well-known problem of estimating autocovariance functions with missing observations, and in our case, for a lack of a better solution, we follow the suggestion of Parzen to obtain an asymptotically unbiased estimate (Priestley 1981, p. 585). Under the assumption of an isotropic distribution, the BT autocovariance becomes a function of the radial distance and time. It is then justifiable to average out the angular contribution by integration to obtain a 1-d BT autocovariance function at the 0th time bin. Theoretically, this represents the autocovariance function of waves having periods more than 5 days (since those waves with periods less than 5 days are averaged out). We describe the above steps more precisely as follows. An estimate of the 3-d spatio-temporal autocovariance function can be obtained as follows. We can write the SSH field as

$$Y(\mathbf{p},t) = g(\mathbf{p},t)X(\mathbf{p},t)$$

where $g(\mathbf{p},t) = 1$ if $(\mathbf{p},t) = (x, y, t)$ lies on a satellite track, and 0 otherwise. The 3-d autocovariance function is then estimated by

$$Cov(x,y,t) = Cov_X(x,y,t) = Cov_Y(x,y,t)/Cov_g(x,y,t).$$

Equivalently, let $S(x,y,t) = \{\sum_{i,j} z_i z_j : x \le \mathrm{dist}(x_i,x_j) < x + \Delta x, y \le \mathrm{dist}(y_i,y_j) < y + \Delta y, t \le |t_i - t_j| < t + \Delta t\}$ and $\#S(x,y,t) = \{\sum_{i,j} 1 : x \le \mathrm{dist}(x_i,x_j) < x + \Delta x, y \le \mathrm{dist}(y_i,y_j) < y + \Delta y, t \le |t_i - t_j| < t + \Delta t\}$, then

$$Cov(x,y,t) = \frac{S(x,y,t)}{\#S(x,y,t)}.$$

Parzen has shown that the above is a consistent estimate and is asymptotically unbiased. By the! assumption of isotropy, a 2-d version of tile above can be obtained by averaging out the angular component

$$Cov(r,t) = \frac{1}{2\pi}\int_0^{2\pi} Cov(r,\theta,t)d\theta,$$

and this gives the l-d between-track autocovariance functions as

$$BTCov(r) = Cov(r,\ 0).$$

It must be mentioned that a satellite travels at a very high velocity (for example 10PEX covers a 1000 km long segment of a track in less than 3 minutes), and hence the AT autocovariance function is more like taking a snapshot of the ground track segment, and the BT autocovariance function is akin to a moving average filtering of the data in the time domain. In fact, if wc take a small synchronicity interval Δt, say 3 minutes, then BTCov coincides with ATCov, as expected. It turns out that for large values of Δt, say 5 days or more, then BTCov and AT Cov differs in the time scale of oceanic motions that they represent, the former describing those slower moving ocean eddies and planetary waves, and the latter that of faster internal gravity waves.

Some nice relationships exist between the spectra of the two types of autocovariance functions (for example, Monin and Yaglom (1975) Sec. 12.2; Fu (1983); Le Traon (1990)). We specifically mention one important case, i.e. for small Δt ($\lesssim$ 3 minutes), the Fourier transform of $Cov(x, y, 0)$, $\mathcal{F}[Cov(x,y,0)] = P_2(k_1, k_2)$, represents the power spectrum of the 2-d SSH random field and under the assumption of isotropy, it is related to the power spectrum E_1 of the l-cl along-t] ack SS11 oscillations by

$$\int_{-\infty}^{+\infty} P_2(k_1,k_2)dk_2 = E_1(k_1). \qquad (1)$$

Now for large values of At, the above equation no longer holds, and the difference between the left hand side and the right hand side gives an indication of the residual energy belonging to the fast internal gravity waves known in ocean literature as baroclinic inertia

gravity (BIG) waves (Glazman 1996). BIG waves travel at phase speeds on the order of 3 m/s, with wavelengths varying from 10 to 1000 km, and have periods not exceeding the inertial period arising from the earth's rotation (less than 24 hrs in the mid-latitude regions). Typical graphs of the decomposition of the ATCov into the 2 components are shown below.

Figure 7 here

Notice the distinctly steeper slope of the spectrum of the between-track component (from -4 to -5), and this is in agreement with the predictions of the geostrophic turbulence theory (Charney 1971) on the power law for Rossby waves. We concentrate on the power spectrum of BIG waves, which contains much information about the physical parameters of the earth's ocean, as we will see below. As an example, we apply the estimates above to compute the Rossby radius of deformation of a particular patch. The Rossby radius is an important quantity in both ocean and atmospheric sciences, for it is the characteristic scale in which rotation effects of the earth become dominant (Gill 1982, p. 205), and is a function of the ocean depth, gravitational pull, and the earth's Coriolis frequency. In the paper (Glazman 1996), the theory of BIG waves is developed and its predicted theoretical spectrum for the direct cascade energy transfer type is given by

$$F(k) = Q(v)\frac{(z-1)^{1/2}(z^2+4v-9)}{(z^2-1)^{(2v-3)/(v-1)}z^{5/2(v-1)}},$$

where $z = 1 + k^2R^2$, k is the wavenumber, R is the Rossby radius, v is an integer denoting the number of wave-wave interactions (degree of nonlinearity), and $Q(v)$ is the energy flux that depends only on v. An estimate of R is immediately obtained from the data by minimizing the least squares fit between the theoretical and observed spectrum. For the Atlantic ocean, these values of R were found to be within reasonable agreement with previous calculations obtained from *in situ* data (Emery, 1/cc, and Magaard 1984; Houry et al 1987), details of which will be presented in a forthcoming paper. The question of how

BIG waves are generated is still not well understood and is currently a subject of intense research in oceanography.

The 3-d spatio-temporal autocovariance functions $Cov(x, y, t)$ contains quite a bit of information about a patch. Looking at 2-d slices of it of the form $Cov(x, 0, t)$ and $Cov(0, y, t)$ provides information about the propagation speed of planetary waves. The prominent elongated shape in the center of the figure below shows the westward movement of a planetary Rossby wave, moving at a speed of around 4 cm/sec (the slope of the shape), typical of such waves in the region (how to obtain efficient estimates of the slope is another statistical problem in its entirety and will be discussed in a future article). Notice the parallel streaks that are approximately a year apart from the central shape, and this indicates that the period of such waves is close to a year.

Figure 3 here

A simple illustration will show why this is so. Assume for simplicity that the wave is a plane wave, with a random phase added to ensure stationarity, that is, $U(x, t) = A\cos(kx - \omega t + \phi)$ *and* $Ee^{i\phi} = 0$. Its phase speed in this case is given by $c = \omega/k$. Then

$$Cov(r, \tau) = E[U(x + r, t + \tau)U(x, t)] = A\cos(kr - \omega\tau)/2,$$

which is no longer random, and whose phase speed ω/k and period *can* now be measured. In actual practice, it is rarely the case that planetary waves mimic plane waves with constant wavenumbers and frequencies. In fact, planetary waves are polychromatic, and the dispersion relationship characterizes the relationship between those quantities, and is equal to (Gill 1982, p. 446):

$$\omega(k) = \frac{-\beta k_x}{k^2 + 1/R^2}, \tag{2}$$

where $k = \sqrt{k_x^2 + k_y^2}$, β depends only on latitude (assumed constant for a patch), and R is the internal Rossby radius. In the case of the zonal slice $Cov(x, 0, t)$, the phase speed

is again c = $\omega(k)/k_x$ which now depends on both k and R. This provides us with another alternative method for determining R once we know the value of the wavenumber k. It must be emphasized that the estimated speed obtained as the slope of the the zonal slices from this technique is only an approximation of the true phase speed to the first order. At first sight, it seems that the FFT of the above autocovariance slices may yield more information on the wave structure. However, this approach did not produce any clear results, due to the complicated nature of the dispersion relationship and the need for greater accuracy in the autocovariance estimates (as is well-known, the unbiased estimate used is not always positive semidefinite. It is suggested that the large gaps in the estimate which are due to uneven coverage of the satellite passes may benefit from better interpolation methods, such as the use of splines, since usual linear interpolation techniques compromises the positive semidefiniteness of the autocovariance function). Some simulations might be helpful, such as building a model of the ?-d spectrum and see if the corresponding inverse FFT reproduces some of tile features observed so far. The following equations show the fundamental relationships between various spectras. Let $\Phi(k_x, k_y, \omega) = \int\int\int Cov(x, y, t) \exp[i(xk_x + yk_y - \omega t)]dk_x\, dk_y dt$ and $\omega = \Omega(k)$ denote the above dispersion relation (2). Then the ?-d spectrum is given by

$$F(k_x, k_y) = \int_{-\infty}^{+\infty} \Phi(k_x, k_y, \omega) d\omega,$$

and the Fourier transform of the slice $Cov(x, 0, t)$ is given by

$$\begin{aligned}
F_x(k_x, \omega) &= \int\int Cov(x, 0, t) \exp[-i(xk_x - \omega t)]dx dt \\
&= \int\int\int\int F(k'_x, k'_y) \exp[i(xk'_x - \Omega(k)t)] \exp[-i(xk_x - \omega t)]dk'_x dk'_y dx dt \\
&= \int\int\int F(k'_x, k'_y)\delta(k'_x - k_x) \exp[i(\omega - \Omega(k))t]dk'_x dk'_y dt \\
&= \int F(k_x, k'_y)\delta(\omega - \Omega(k_x, k'_y))dk'_y \\
&= F\left(k_x, \sqrt{\frac{-\beta k_x}{\omega} - \frac{1}{R^2} - k_x^2}\right).
\end{aligned}$$

Similarly, one can show that

$$F_y(k_y,\omega) = F\left(\frac{-\beta + \sqrt{\beta^2 - 4\omega(k_y^2 + 1/R^2)}}{2\omega}, k_y\right).$$

The above equations illustrate the important point, that the 2-d wavenumber-frequency spectra can be obtained from the 2-d wavenumber spectra alone.

Equation (1) also has an interesting interpretation viewed from the perspective of computer tomography. It says that the along-track spectrum are the sum-total of contributions of 1-d slices of the 2-d spectrum. Utilizing the isotropy assumption, we can recover the full 2-d AT wavenumber spectrum via techniques in tomography, such as the filtered back-projection algorithm (Kak and Slaney 1988). By our results above, both the 2-d AT wavenumber-frequency spectrum and spatio-temporal autocovariance can also be recovered and analyzed, a subject of current research.

Finally, one can look at the FFT of the whole 3-d spatio temporal autocovariance function, and our preliminary investigations indicate that the 3-d wavenumber-frequency spectrum contain enough interesting "features that merits further exploration in the future.

3. Some Applications of 3rd and Higher Order Statistics

Up to now, nothing has been said about the nature of the distribution of the SSH random field. Most authors would prefer to take the simplest case and assume that the distribution is a priori Gaussian. A check of the along-track 3rd order cumulant $\mathrm{Cum}(\|\mathbf{r}\|, \|\mathbf{s}\|) = \mathrm{E}(X(\mathbf{p})X(\mathbf{p}+\mathbf{r})X(\mathbf{p}+\mathbf{s}))$ for the same patch above shows no significant deviation from zero at the 95% confidence level, including the origin which gives the 3rd moment (skewness) $\mathrm{Cum}(0,0)$. The test statistic used was the standard $\sqrt{n}$ times sample mean divided by the sample standard deviation for each 6 km by 6 km cell (the resolution plot), where $n = 73$ is the number of realizations, and the absolute value of the test statistic is uniformly less than 1.2742 everywhere. Standard application of the CLT does not reject the null hypothesis that the 3rd order cumulant is significantly different

from zero. of course this doesn't prove anything about the distribution of the SSH field, except to show that there arc no significant 3- wave interactions for this particular patch. However, other patches we have tested did not exhibit similar behavior. For example, for a patch in the South Atlantic with coordinates longitude 340,350 and latitude -25,-15, the value of the test statistic is 3.7324 for the 3rd moment, with 8 other points significantly greater than 2 in a 600 km x 600 km lag space. An appropriat c model therefore for this SSH field is of the form

$$X(\mathbf{p}) \; X_0(\mathbf{p}) + X_g(\mathbf{p}),$$

where X_0 and X_g represents the non - gaussian and gaussian component respectively, both independent of one another. Recovery of the non-gaussian signal can be accomplished by using the bispectrum signal reconstruction technique popular in electronic speech and imaging applications (Nikias and Petropulu 1 993). let $C_3(k_1, k_2)$ denote the bispectrum of X, which is the Fourier transform of the 3rd order cumulant Cum($\|\mathbf{r}\|, \|\mathbf{s}\|$). Then the phase $\phi_0(k)$ and magnitude $\|F_0(k)\|$ of t he spectrum of X_0 is given by (Nikias and Petropulu 1993,p. 235)

$$\phi_0(k) = \frac{1}{2n+1} \sum_{i=-n}^{n} \Psi(k,i),$$

$$\|F(k)\|^2 = \alpha \exp\left(\frac{1}{2n+1} \sum_{i=-n}^{n} \ln \|C_3(k,i)\|^2 \right),$$

where $\Psi(k_1, k_2) = \arg(C_3(k_1, k_2))$ and α is a posit ive constant. It is clear that since the 3rd order cumulants of X_g vanishes, t he reconstruct ed signal belongs to the non-gaussian component of X. Graphs of the magnitude an d phase of the recovered signal X_0 are shown below.

Figure 4 here

Wc note that those values whose wavenumbers lie beyond .3 rad/km are in the noise range of the altimeter, hence not to be trusted. That the phase is non-zero indicates that the

signal is spatially inhomogeneous. We are in the process of investigating what kind of oceanic processes would give rise to this non gaussian non-homogeneous signal, though we speculate that the signal is dominated by eddies and 2-d turbulence. More patches also need to be tested to determine where in the ocean are such signals prevalent. One could also compute the between-track 3rd order cumulant using similar techniques as in the computation of BT autocovariance function, but because of its complexity, we leave this open for future investigations.

If the SSH field is determined to have a significant 3rd order cumulant, then we can compute the bicoherency function, which is the normalized magnitude of the bispectrum, and use it to measure the degree of phase coupling between triads of waves (Hasselman, Munk, arid MacDonald 1963). In addition, it was shown in (Masuda and Kuo 1981) that the biphase, which is the phase of the bispectrum, is related to the shape of the original field X. These two quantities can be computed as follows:

$$B(k_1, k_2) = \frac{\|C_3(k_1, k_2)\|}{\|F(k_1)F(k_2)F(k_1 + k_2)\|}$$

$$\beta(k_1, k_2) = \arctan\left[\frac{-\mathrm{Im}(C_3(k_1, k_2))}{\mathrm{Re}(C_3(k_1, k_2))}\right].$$

However, duc to the low signal-to-noise ratio observed in the 3rd order cumulants for the above patches, the results have so far been inconclusive. We have identified 4 possible mechanism for which wave couplings can occur in the scales under consideration. Planetary waves, BIG waves, resonant interaction between planetary and BIG waves, and 2 dimensonal geostrophic turbulence all give rise to triad interactions. 'There is also a need to distinguish which type of mechanism are responsible for the couplings once they are observed. Wc also note that in (Glazman 1996), it is theorized that 4-wave interactions are far more prevalent between BIG waves, hence it is an intriguing application to use trispectral analysis to verify this. However, this would seem to require another major improvement in remote sensing technology, as the increased noise level would have drowned the signal all too easily, plus the computational resources required to compute the 4th

order cumulant and trispectra are somewhat forbidding compared to the above.

4. Conclusions

Satellite remote sensing technology have advanced to the stage where it is now possible to do higher order statistics with big)] precision. The 1- d and 2-d autocovariance functions were used to provide evidence that BIG waves exists in the open ocean, while 3rd order statistics indicate the non-gaussian inhomogeneous nature of the signal, as well as the possible wave couplings that may occur at the mesoscale domain. The above techniques can also be applied to validate ocean models by cross- checking the results computed with a model with those obtained from the satellite altimeter. In the years ahead, we foresee that satellite remote sensing will become n 101 e and more common, having already replaced the ocean-faring research vessel as the defact o standard for collection of oceanographic data. Technological progress have made them economically cheaper and are astonishing in their capability to haul in huge chunks of global data that a r c magnitudes greater in comparison to in situ methods, 1 Research are c urrently conducted to inc. corporate even more oceanographic variables that ar c not currently accessible to satellite detection, and all this would require the use of advance statistical procedures to process the resulting information for human consumption.

References

Benada, R. (1993), *PO.DAAC Merged GDR(TOPEX/Poseidon) Users Handbook,* Version 1.0, 1993.

Charney, J.G. (1971), " Geostrophic Turbulence," *Journal of Atmospheric Sciences, 28,* pp. *1087-1095.*

Chelton, D.B., W.F. Eddy, R. 1 Deveaux, R. Feldman, R.E. Glazman, A. Griffa, K.A. Kelly, G. MacDonald, M. Rosenblatt , B. Rozovskii, J. Tucker (1 994), " Report 011 Statistics and Physical Oceanography," *Statistical Science,*9,pp. 167-221.

Emery, W. J., W.G. Lee, and L. Magaard (1984), " Geographic and Seasonal Distributions of Brunt-Väisälä Frequency and Rossby Radii in the North Pacific and North Atlantic," *Journal of Physical Oceanography,* 14, pp. 29.431 7.

Fu, L.L. (1983), "On the Wave Number Spectrum of Oceanic Mesoscale Variability Observed by the SEASAT Altimeter," Journal *of Geophysical Research,* 88, (C7), *pp. 4331-4341.*

Fu, 1,.1,., E.J. Christensen, C.A. Yamarone Jr., M. Lefebvre, Y. Menard, M. Dorrer, and P. Escudier (1994), " TOPEX/Poseidon Mission Overview," *Journal of Geophysical Research,* 99, (C12), pp. 24369-24381 .

Gill, A. Il. (1982), Atmosphere-Ocean Dynamics, Academic Press, NY.

Glazman, R.E. (1986), " Statistical Characterization of Sea Surface Geometry for a Wave Slope Field Discontinuous in the Mean Square," *Journal of Geophysical Research,* 91, (C5), pp. 6629-6641.

Glazman, R.E. (1 996), " Scale-dependent Ocean Wave Turbulence," in Stochastic *Models in Geosyst ems,* eds. S.A. Molchanov and W. Woyczynski, IMA Volumes in Mathematics and Applications, 85, Springer Verlag, NY, pp. 97-114.

Glazman, R. E., A. Fabricant, and A. Greysukh (to appear in June, 1996), "Statistics of Spatio-temporal Variations of Sea Surface Height based on TOPEX Altimeter Measurements," *International Journal of Remote Sensing.*

Hasselman K., W. Munk, and G. MacDonald (1963), " Bispectra of Ocean Waves, " Time Series *Analysis,* ed. M. Rosenblatt, John Wiley, NY, pp. 125-139.

Houry S., E. Dombrowsky, P. DeMey, and J P. Minster (1987), "Brunt-Väisälä Frequency and Rossby Radii in the South Atlantic," *Journal of Physical Oceanography,* 17, pp. 1619-1626.

Kak, A. C. and M. Slaney (1988), Principles of Computerized Tomographic Imaging, IEEE Press, New York.

LeBlond, P.H. and L.A. Mysak (1978), Waves in the Ocean, Elsevier, Amsterdam.

Le Traon, P.Y. and M.C. Rouquet (1990). "Spatial Scales of Mesoscale Variability in the North Atlantic as Deduced from Geosat Data," *Journal of Geophysical Research*, 95, (C1 1), pp. 20267-20285.

Masuda A. and Y.Y. Kuo (1981), "A Note on the Imaginary Part of Bispectra," *Deep-Sea Research*, 28A, (3), pp. 213 222.

Monin, A.S. and A.M. Yaglom (1975), Statistical Fluid Mechanics, Vols. I, II, MIT, Cambridge.

Nikias, C.L. and A. Petropulu (1993), Higher Order Spectra Analysis, Prentice Hall, New Jersey.

Phillips, O.M. (1977), The Dynamics of the Upper Ocean, Cambridge university Press, New York.

Priestly, M.B. (1981), Spectral Analysis and Time Series, Vol.1, Academic Press, London.

Rosenblatt, M. (1985), Stationary Sequences and Random Fields, Birkhäuser, Boston.

Wunsch, C. and A.E. Gill (1976), "Observations of Equatorially Trapped Waves in the Pacific Sea Level Variations," *Deep-Sea Research*, 23, pp. 371-390.

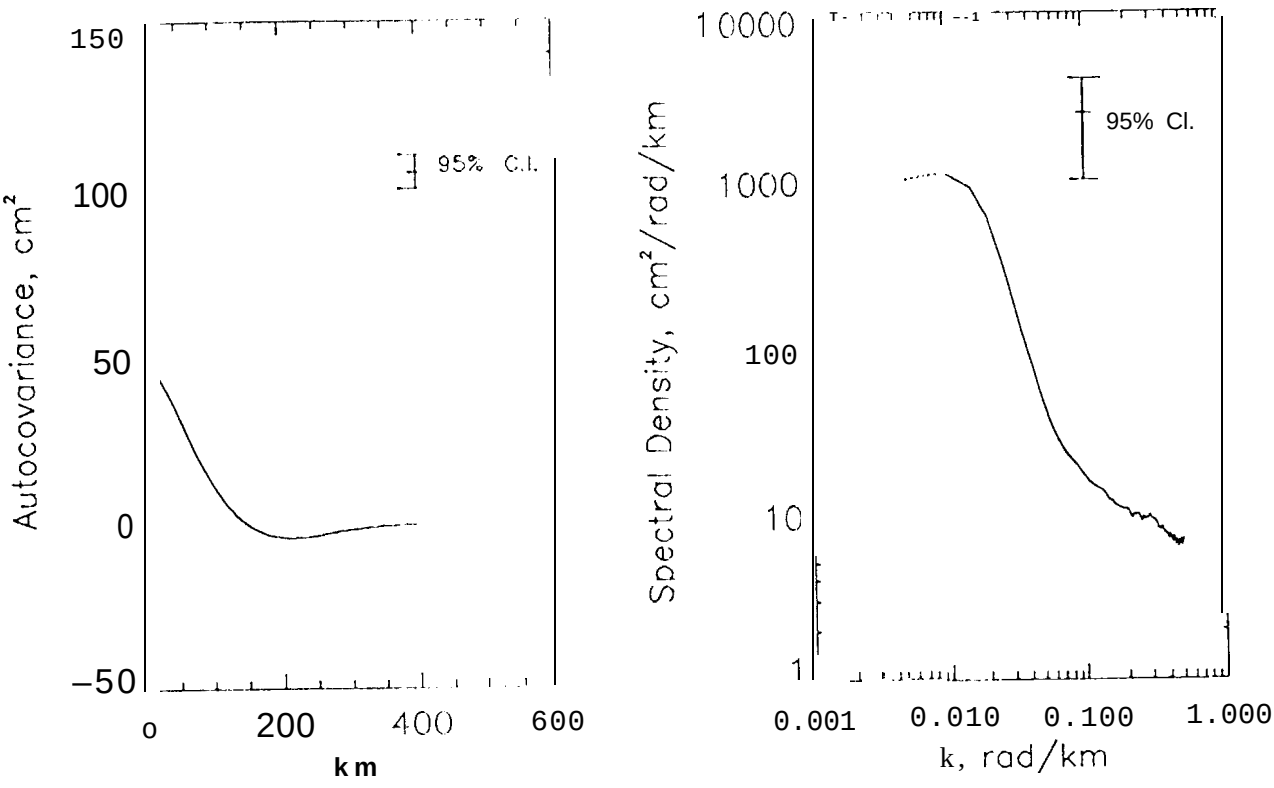

Figure 1. **The AT** autocovoriance func tion **ond** its spectrum, computed from **a patch in the** North Atlantic ocean, **Longitude 320-330, Latitude 30–40.**

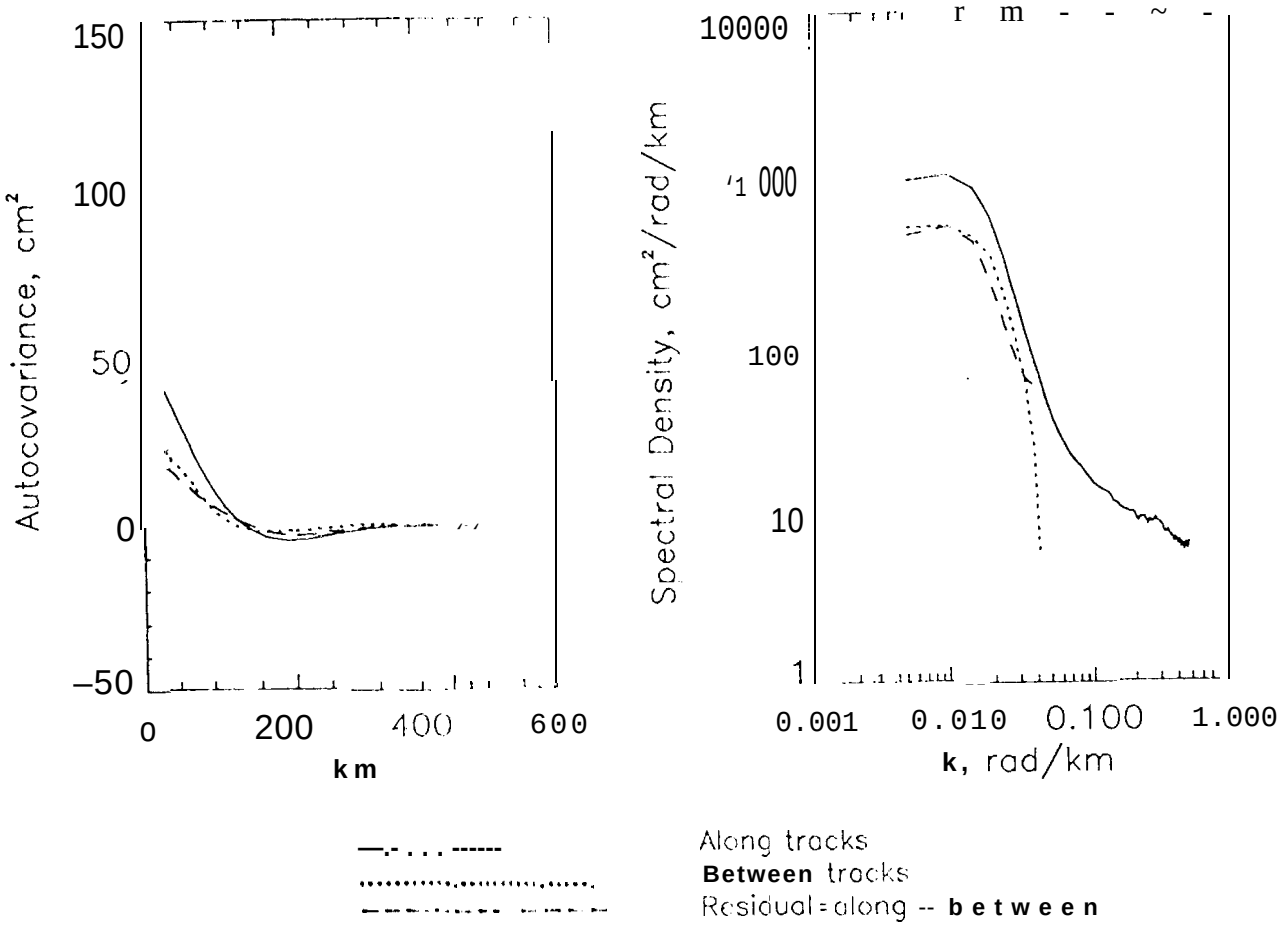

Figure 2. Decomposition of the Al autocovariance and **spectrum into the BT ond BIG** components.

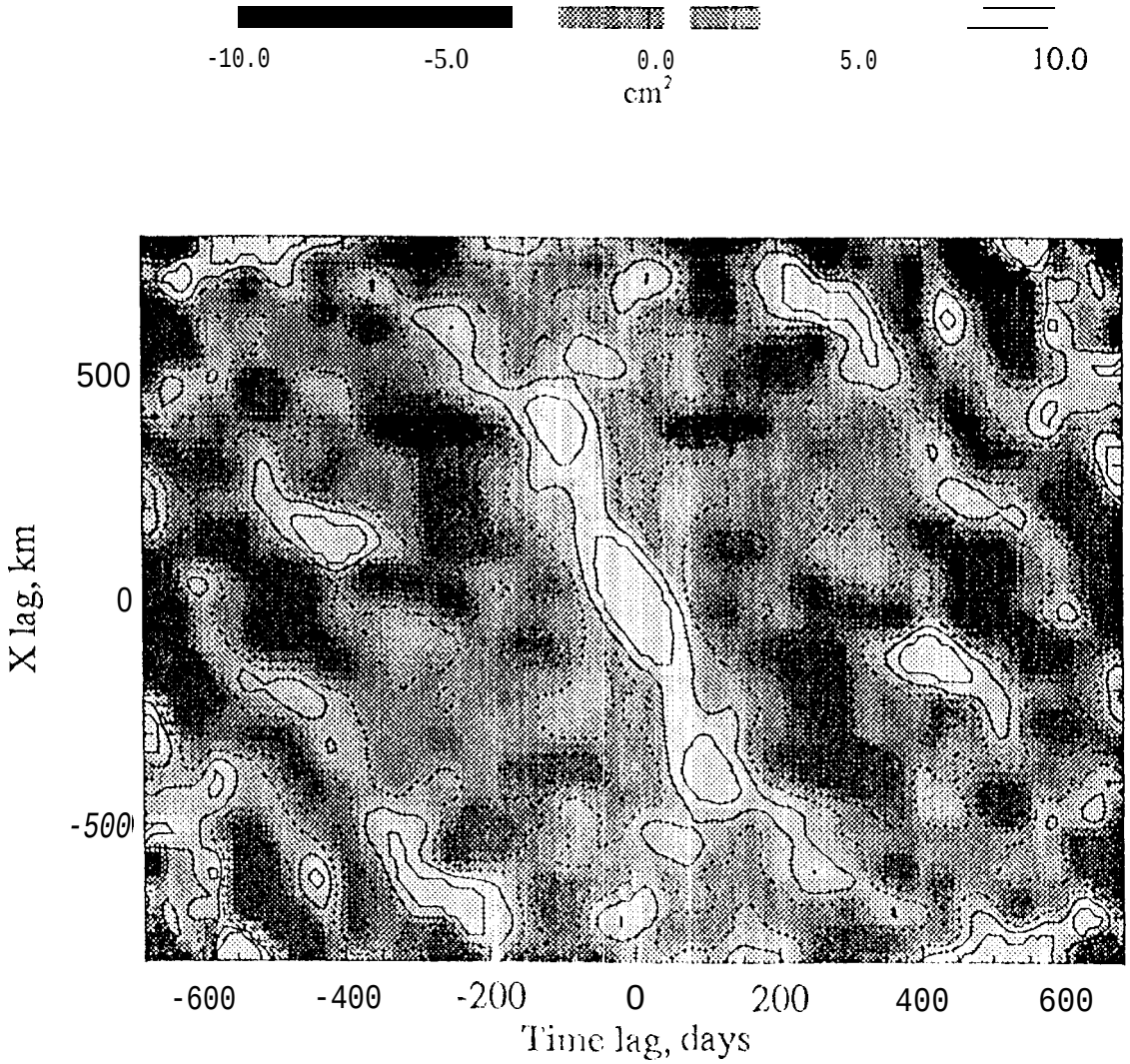

Figure 3. BT Autocovariance function

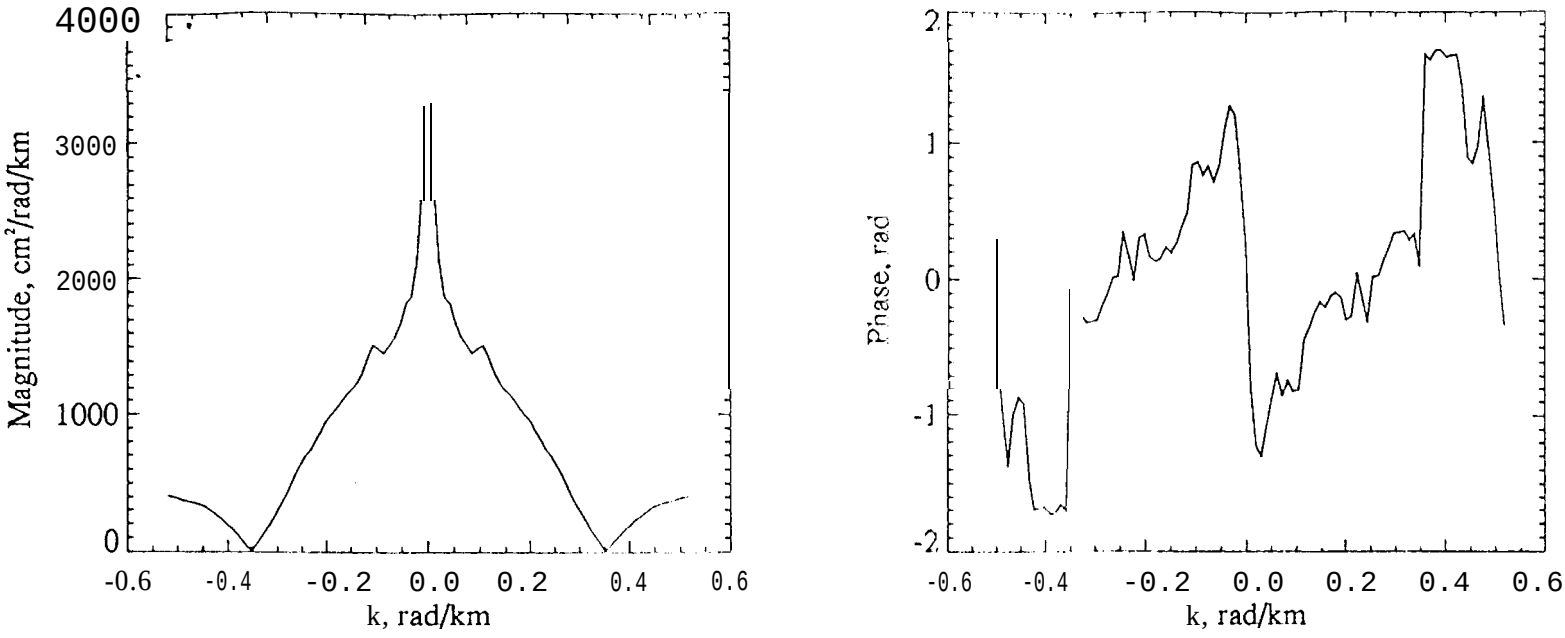

Figure 4. The magnitude and phase of the spectrum of XO